

**NASA
Technical
Paper
2791**

1988

An Analytical Study of
the Hydrogen-Air Reaction
Mechanism With Application
to Scramjet Combustion

Casimir J. Jachimowski

*Langley Research Center
Hampton, Virginia*



National Aeronautics
and Space Administration

Scientific and Technical
Information Division

Introduction

An important element in the National Aero-Space Plane (NASP) research program at the Langley Research Center is the development of the analytical tools or models that are needed for analyzing and gaining insight into the combustion problems associated with propulsion systems required to operate at flight speeds up to Mach 25. Recently, special attention has focused on the role that chemical kinetic effects can have on the performance of high Mach number combustion systems. Mechanisms describing the detailed chemical kinetics of hydrogen oxidation have been developed by a number of authors, and many of these mechanisms have been reviewed by Dougherty and Rabitz (1980). In the present paper a detailed chemical kinetic mechanism for the combustion of hydrogen is presented and discussed. The purpose of this study was to assemble a chemical mechanism that reproduced, with reasonable accuracy, the observed behavior of the hydrogen-air system as determined in shock-tube studies and in laminar flame studies. A second objective was to examine the effect of chemical kinetics on combustion at representative scramjet combustor conditions. Particular attention was given to the effect of uncertainties in the rate coefficients on the calculated ignition delay times, burning velocities, and combustor performance.

Symbols

A/A_o	area ratio along combustor
a	constant in mixing schedule equation
\bar{D}	self-diffusion coefficient for molecular oxygen
D_{ij}	binary diffusion coefficient for species i and j
F_i, F_j	diffusion factors for species i and j
k_j	rate coefficient for reaction j
M	flight Mach number
MW_i	molecular weight of species i
p	pressure, atm
R	universal gas constant
T	absolute temperature, K
V	initial velocity at combustor entrance
η_{mix}	mixing efficiency
η_{ck}	chemical kinetic efficiency
ϕ	fuel-air equivalence ratio

Hydrogen-Air Reaction Mechanism

In the assembly of the reaction mechanism, reactions were included that involve all the important species in the hydrogen-oxygen system— H_2 , O_2 , H , O , OH , H_2O , HO_2 , and H_2O_2 . In addition, reactions were included for the species N , NO , and HNO , which may become important in the hydrogen-oxygen-nitrogen system at the high Mach number conditions ($M > 12$). The proposed hydrogen-air combustion mechanism and rate coefficients are given in table I. The reactions in the mechanism are based for the most part on the reactions and rate coefficients recommended by Baulch et al. (1972), Baulch, Drysdale, and Horne (1973), Dixon-Lewis and Williams (1977), Dixon-Lewis (1979), and Dougherty and Rabitz (1980). The third-body efficiencies were taken from Gay and Pratt (1971) and Dixon-Lewis (1979). The rate coefficient expressions assigned to reactions (2) and (9) represent values, optimized from this study, that gave the best overall agreement between calculated kinetic results and experimental data. The refinement of the hydrogen-air reaction mechanism is discussed in the next section.

Mechanism Evaluation and Refinement

The hydrogen-air reaction mechanism was refined and evaluated through comparison of calculated kinetic results with experimental data. The refinement involved the adjustment of the rate coefficients for certain reactions to obtain the best agreement with experimental data. The experimental data selected for the comparison were the shock-tube ignition delay data reported by Slack (1977), the laminar burning velocity data assembled by Warnatz (1981), and the laminar burning velocity data reported by Milton and Keck (1984). These data were selected for the comparison because they were obtained from experiments with "real" hydrogen-air mixtures as opposed to diluted or simulated hydrogen-air (e.g., H_2 - O_2 -Ar) mixtures.

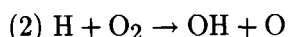
Comparison With Shock-Tube Data

Slack (1977) measured ignition delay times behind the reflected shock for stoichiometric hydrogen-air mixtures near the second explosion limit and for stoichiometric mixtures containing small amounts of nitric oxide. The data selected for the comparison included the ignition delay data at pressures of 0.5, 1.0, and 2.0 atm for stoichiometric hydrogen-air mixtures and the ignition delay data at 2.0 atm for stoichiometric hydrogen-air mixtures containing 0.50 and 2.25 percent nitric oxide. To compare the kinetic behavior predicted by the reaction mechanism with the experimental results, numerical

simulation of the shock-tube experiments was carried out with the computer code described by McLain and Rao (1976). To simulate the conditions behind the reflected shock wave, the code was operated in a constant-volume mode. The ignition delay time was defined as it is in the shock-tube experiments; that is, it was defined to be the elapsed time between the heating of the gas mixture by the reflected shock wave and the sudden pressure increase due to combustion.

The rate coefficients for the reverse reactions in the mechanism were calculated within the computer code with the forward rate coefficients given in table I and the appropriate thermochemical data. The thermochemical data for the hydrogen, oxygen, and nitrogen species were taken from the JANAF (1971) tables.

The calculated ignition delay times were very sensitive to the rate coefficients assigned to reactions (2) and (9),



particularly for the 2.0-atm condition. The sensitivity of the calculated ignition delay times to reactions (2) and (9) is illustrated by the results shown in figure 1. The solid curve in this figure was computed with the rate coefficients listed in table I, and the dashed curves were computed with the altered rate coefficients noted on the figure. Calculated burning velocities (discussed subsequently) were also very sensitive to these rate coefficients, particularly for some rich mixtures. The rate coefficients initially assigned to reactions (2) and (9) were taken from Baulch et al. (1972). Baulch recommended $k_2 = 2.2 \times 10^{14} \exp(-16800/RT)$ with an uncertainty of ± 50 percent for the temperature range 300 to 2000 K. The best overall agreement between the calculated and experimental results was obtained with the rate coefficients for reactions (2) and (9) given in table I. The adjusted rate coefficient for reaction (2) was 18 percent larger than the recommended rate coefficient, and the adjusted rate coefficient for reaction (9) was 5 percent larger than the recommended rate coefficient. The adjusted expressions were within the accepted uncertainty for the reactions.

The results of the computer simulations of the shock-tube experiments for stoichiometric hydrogen-air mixtures at 0.5, 1.0, and 2.0 atm are given in figures 2(a) to 2(c) together with the corresponding experimental results. The calculated ignition delay times were within 20 percent of the experimental

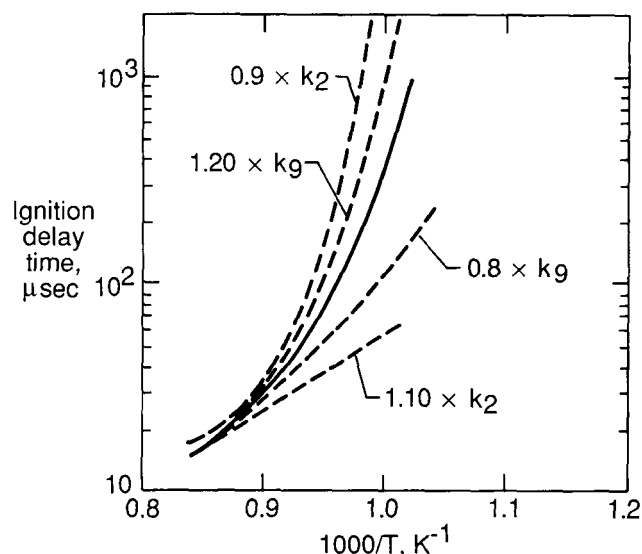
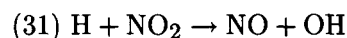


Figure 1. Sensitivity of calculated ignition delay times to rate coefficients for reactions (2) and (9).

results over the entire range of temperatures and pressures examined.

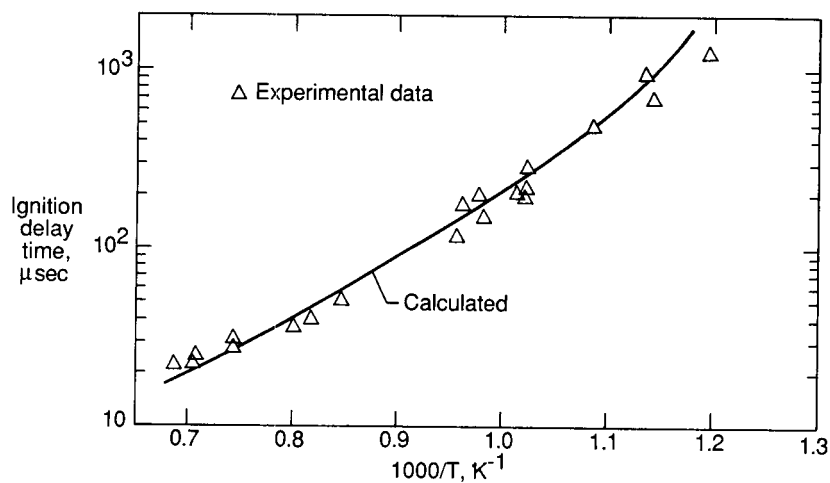
At high flight Mach numbers ($M > 12$), reactions involving nitric oxide are important. Slack and Grillo (1977) investigated the effect of nitric oxide addition on the ignition of stoichiometric hydrogen-air mixtures and determined that the presence of small amounts of nitric oxide (less than 5 percent) reduced the ignition delay times. The high-temperature chemistry of the nitrogen-oxygen system is represented in the mechanism by reactions (20) to (32). The experimental results of the study at 2.0 atm for the addition of 0.5- and 2.25-percent nitric oxide are given in figure 3 together with the results calculated with the proposed reaction mechanism. The agreement between the calculated and experimental results is good. The sensitizing effect of the nitric oxide is primarily due to



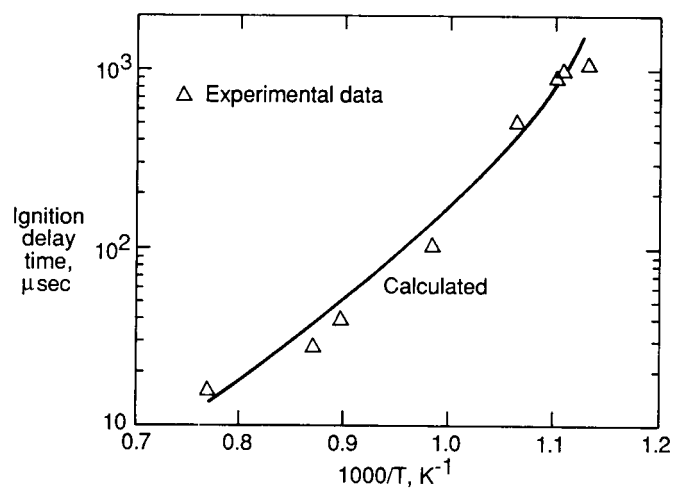
which convert the HO_2 , a chain-terminating species during the ignition delay period, to the very reactive OH radical. The rate coefficients assigned to reactions (22) to (33) were based primarily on the expressions recommended by Slack (1977) and adjustments were not required.

Comparison With Burning Velocity Data

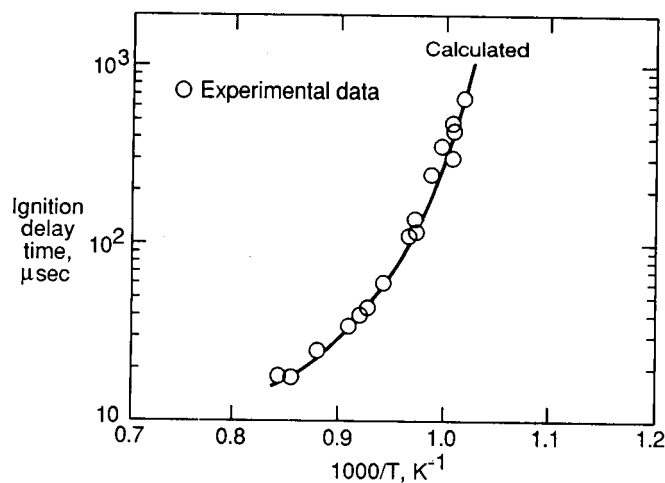
The ability of a reaction mechanism to adequately predict burning velocities is an important, and generally more comprehensive, test of the mechanism at conditions more representative of a combustion environment. The data selected for the comparison



(a) $p = 0.5$ atm.



(b) $p = 1.0$ atm.



(c) $p = 2.0$ atm.

Figure 2. Calculated ignition delay times compared with experimental results for stoichiometric H_2 -air mixtures.

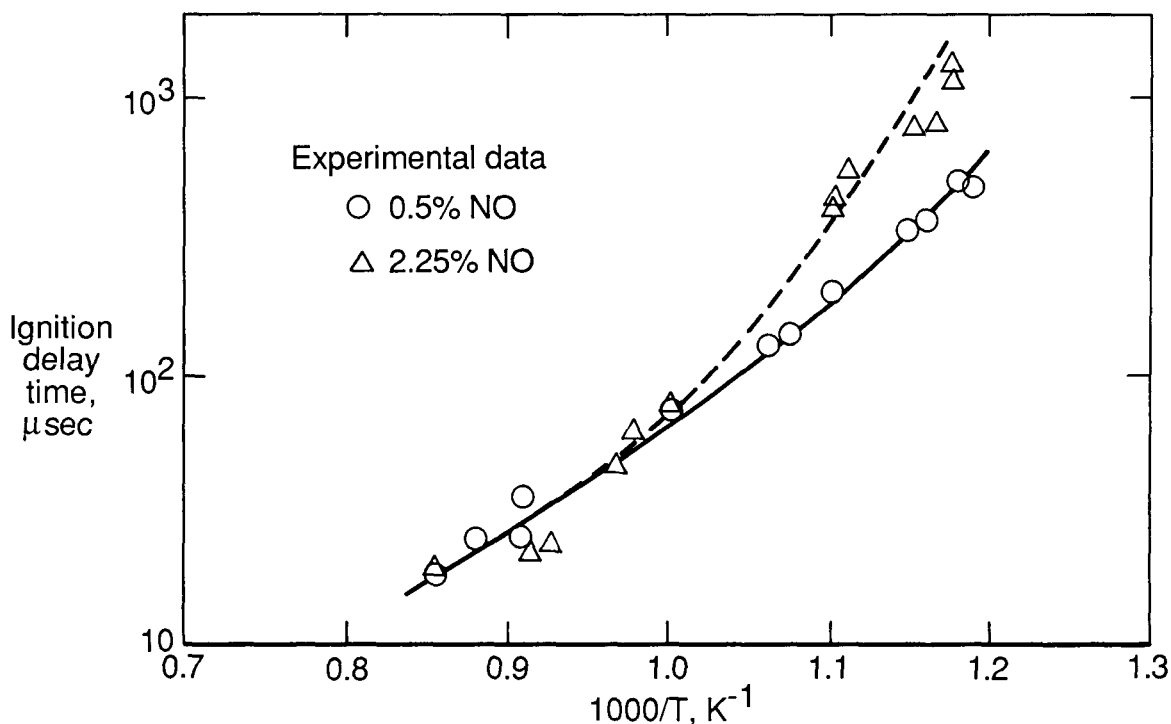


Figure 3. Calculated ignition delay times compared with experimental results for stoichiometric H₂-air mixtures containing nitric oxide. $p = 2.0$ atm.

were the burning velocities assembled by Warnatz (1981) for hydrogen-air flames at pressures of 1 atm and an initial temperature of 298 K for equivalence ratios between 0.5 and 6.0. The burning velocity data reported by Milton and Keck (1984) for stoichiometric hydrogen-air mixtures at temperatures up to 515 K and pressures up to 7 atm were also used. Burning velocities were calculated with the premixed one-dimensional flame (PROF) code developed originally by Kendall and Kelly (1978) for premixed, laminar, laterally unconfined flames. The PROF code models the axial diffusion of heat and species, as well as the chemical kinetic processes, that occur within a one-dimensional flame. The code treats each reaction as reversible and calculates the rate coefficient for the reverse reaction using the forward rate coefficient and the appropriate equilibrium constants. The thermochemical data were obtained from the JANAF (1971) tables.

The governing equations in the flame model are developed through integration of the steady-state two-dimensional species, momentum, and energy equations across a plane perpendicular to the axis. This results in a set of one-dimensional flame equations in terms of bulk gas properties. Species transport equations in the code use binary diffusion coefficients D_{ij} , which are approximated by the empirical relation

$$D_{ij} = \frac{\bar{D}}{F_i F_j}$$

where \bar{D} is a reference self-diffusion coefficient and F_i and F_j are diffusion factors for species i and j . Pressure and temperature dependence of D_{ij} are incorporated into \bar{D} so that F_i and F_j are independent of temperature and pressure. The reference species is molecular oxygen, for which

$$\bar{D} = 1.7 \times 10^{-5} T^{1.659} p^{-1} \text{ cm}^2 \text{ sec}^{-1}$$

where the pressure and temperature are in atmospheres and kelvins. The diffusion factor for species i is determined from the empirically derived relation

$$F_i = (\text{MW}_i/26)^{0.461}$$

where MW_i is the molecular weight of species i . Additional details on the development of the binary diffusion coefficient relation are given in Kendall and Kelly (1978) and Bartlett, Kendall, and Rindal (1968).

As noted previously, burning velocity data were also used to evaluate and optimize the proposed hydrogen-air reaction mechanism. The data used for this purpose were those compiled by Warnatz (1981) for various hydrogen-air mixtures for a pressure of 1.0 atm and an unburned gas mixture temperature

of 298 K. These data are shown in figure 4 together with curves that illustrate the sensitivity of the calculated burning velocities to various reactions. The initial mechanism (without any adjustments to the rate coefficients for reactions (2) and (9)) correctly predicted the position of the maximum burning velocity (H_2 mole fraction ≈ 0.4) but underpredicted the actual value by almost 20 percent. Sensitivity studies with the mechanism showed that the value of the maximum burning velocity was most sensitive to the rates of reactions (2) and (9) and, to a lesser extent, to the net rate of the HO_2 -consuming reactions (10) to (15):

- (2) $H + O_2 \rightarrow OH + O$
- (9) $H + O_2 + M \rightarrow HO_2 + M$
- (10) $HO_2 + H \rightarrow H_2 + O_2$
- (11) $HO_2 + H \rightarrow OH + OH$
- (12) $HO_2 + H \rightarrow H_2O + O$
- (13) $HO_2 + O \rightarrow O_2 + OH$
- (14) $HO_2 + OH \rightarrow H_2O + O_2$
- (15) $HO_2 + HO_2 \rightarrow H_2O_2 + O_2$

The importance of the chemistry of the HO_2 radical in the reaction mechanism is illustrated in figure 4. When the rate coefficient for reaction (9) was decreased by a factor of 10, effectively cutting off the production of the HO_2 radical, the calculated burning velocities were significantly smaller than the experimental data. In the hydrogen-air flame the HO_2 radical is a very important species in promoting flame propagation through reaction (11), which generates the hydroxyl radical OH . The hydroxyl radical then reacts with the molecular hydrogen through reaction (4):

- (11) $HO_2 + H \rightarrow OH + OH$
- (4) $OH + H_2 \rightarrow H_2O + H$

The results of the sensitivity studies with the simulated shock-tube and flame experiments indicated that the best agreement between the calculated results and experimental data could be achieved by a simultaneous increase in the rate coefficients for reactions (2) and (9) while the rate coefficients for reactions (10) to (15) were kept fixed. Adjustments to the rate coefficients were kept within the reported uncertainty limits. The solid curve shown in figure 4 represents the burning velocities calculated with the mechanism listed in table I. The mechanism correctly predicted the position of the maximum burning velocity and the calculated values were within 5 percent of the experimental data.

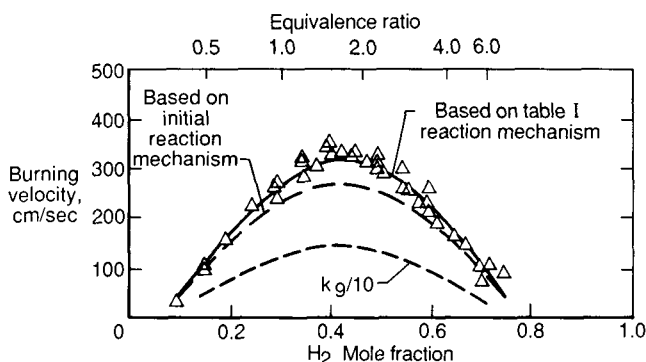


Figure 4. Calculated burning velocities compared with experimental data for H_2 -air mixtures at $p = 1.0$ atm and unburned gas temperature of 298 K.

The results shown in figures 5 to 7 are comparisons of calculated burning velocities with the data reported by Milton and Keck (1984). Milton and Keck measured laminar burning velocities for stoichiometric hydrogen-air mixtures using a spherical constant-volume combustion bomb which gave results over a range of unburned gas temperatures and pressures. The results shown in figure 5 illustrate the effect of the initial unburned gas temperature on the burning velocity for a stoichiometric mixture at $p = 1.0$ atm. The calculated results were in good agreement at 300 K and about 20 percent higher at 400 K. The results shown in figure 6 illustrate the effect of pressure on the burning velocity at an unburned gas temperature of 298 K. The calculated results were within 8 percent of the experimental data.

Most of the hydrogen-air burning velocity data generated by Milton and Keck (1984) were for a range of unburned gas temperatures and pressures. These results fall within the data band shown in figure 7. The calculated burning velocities were in good agreement with the experimental results for pressures up to about 5.0 atm. At higher pressures the experimental burning velocities were up to 15 percent larger than the calculated results. Attempts to provide better agreement at the higher pressures (by varying rate coefficients) without affecting the results at other conditions were not successful. No explanation can be offered for the difference between the calculated and experimental results at the high pressures and temperatures.

Application to Scramjet Combustion

Calculations have been carried out to examine the effect of chemical kinetics on combustion at representative scramjet combustor conditions. The combustor conditions that were considered correspond to flight Mach numbers of 8, 16, and 25. The mathematical model used in this study was based on a

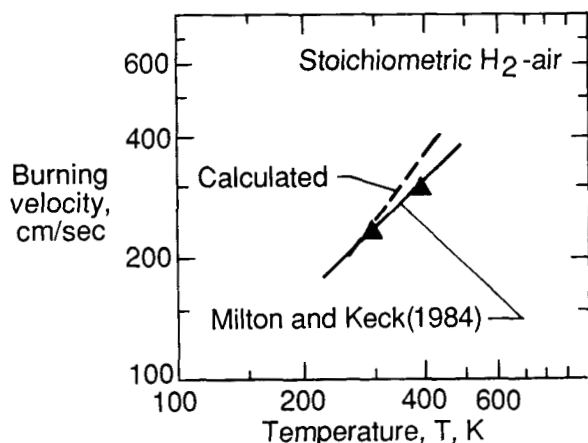


Figure 5. Comparison of calculated burning velocities with experimental results for $p = 1.0$ atm.

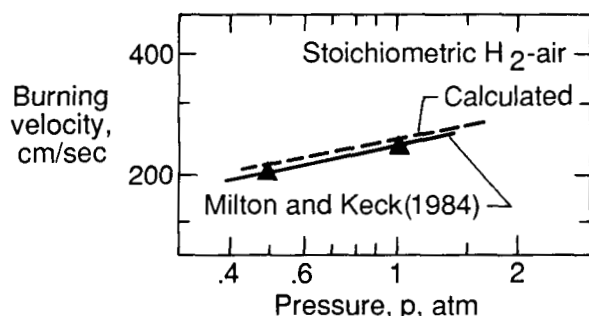


Figure 6. Comparison of calculated burning velocities with experimental results for $T = 298$ K.

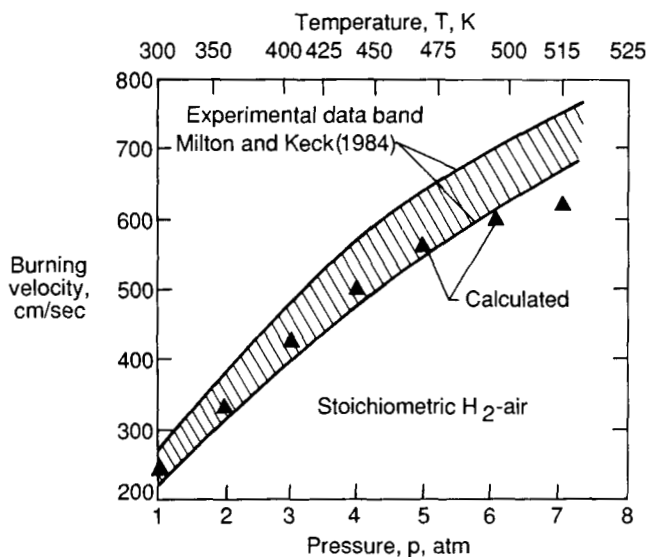


Figure 7. Comparison of calculated burning velocities with experimental results for range of temperatures and pressures.

one-dimensional flow reactor which solved the mass, momentum, and energy conservation equations for

a steady flow system. The model was based on the computer codes described by Bittker and Scullin (1972) and McLain and Rao (1976) and was capable of treating reactions in a flowing system with variable geometry. To simulate the combustion process it was assumed that at the entrance to the combustor the hydrogen, air, and any ignition source constituents are in thermal equilibrium but not fully mixed on a microscale. A mixing routine was included in the model, which allowed the unburned fuel and air to be mixed at a prescribed schedule along the combustor. The fuel and air were mixed; they were then permitted to react. The mixing schedule was fixed to maintain a stoichiometric reaction zone until either the fuel (when $\phi < 1$) or the air (when $\phi > 1$) was fully mixed.

The conditions at the entrance to the combustor are given in table II for the three flight Mach numbers examined. Column T is the temperature of the hydrogen-air mixture and V is the initial velocity of the mixture. These initial conditions are for a combustor in which the fuel is injected perpendicular to the direction of the air flow. The combustor geometry associated with each flight Mach number is shown in figure 8 in terms of the combustor area distribution. Each combustor configuration had two sections with different area distributions. The first section was 50 cm long and the second section was 100 cm long. Even though the configurations in figure 8 have been referred to as a combustor, subsequent discussions in this report refer to the first section as the combustor section and the second section as the nozzle section.

The assumed mixing schedules for each condition are shown in figure 9. The mixing schedule was input into the computer code in the form $\eta_{\text{mix}} = 1 - \exp(-ax)$, where a is a constant, x is the distance in centimeters, and η_{mix} is the mixing efficiency. The mixing schedule was obtained from a correlation developed by Anderson and Rogers (1971) and by Anderson (1974). The correlation, which is a function of fuel-air equivalence ratio and fuel injector spacing, was based on experimental results from studies of cold flow mixing. When the overall equivalence ratio is less than or equal to one, the mixing efficiency η_{mix} is defined as the fraction of total hydrogen that has been mixed with a stoichiometric amount of air and allowed to react. When the equivalence ratio is greater than one, the mixing efficiency is defined as the fraction of total air that has been mixed with a stoichiometric amount of hydrogen.

The effect of chemical kinetic factors on the combustion process was evaluated by comparison of the calculated specific internal thrust for the case in which the combustion chemistry was described by

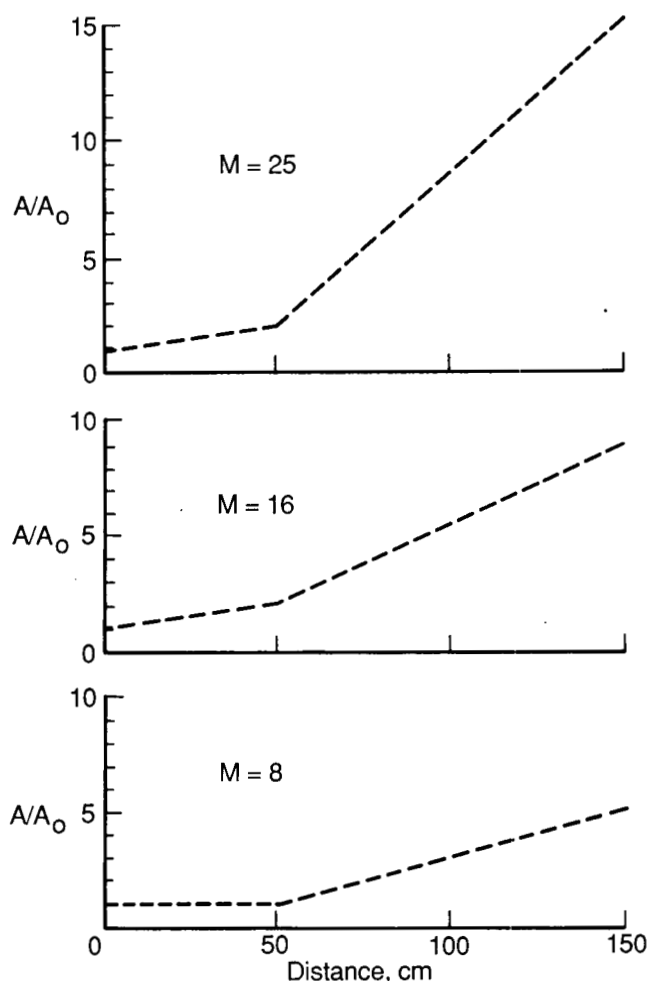


Figure 8. Combustor area distributions.

nonequilibrium chemistry with that for the case in which the combustion chemistry was described by equilibrium chemistry. The specific internal thrust is defined as the internal thrust divided by the total mass flow of fuel and air. The results of the study are expressed in terms of the ratio of the internal thrust for the nonequilibrium case to the internal thrust for the equilibrium case. In this report this ratio is called the chemical kinetic efficiency η_{ck} .

The results of the initial studies for the Mach 8 condition revealed that self-ignition of the hydrogen-air mixture did not occur and that an ignition source was needed. Consequently a study was carried out to determine what effect the quantity of the ignition source had on the combustion process. The results of this study are shown in figure 10, in which the chemical kinetic efficiency is plotted against the ignition source fraction. When the equivalence ratio is less than or equal to one, the ignition source fraction is defined as the fraction of the total moles of hydrogen that is allowed to react to equilibrium with a stoichiometric amount of air and to act as an ignition source for the remaining hydrogen and air. When

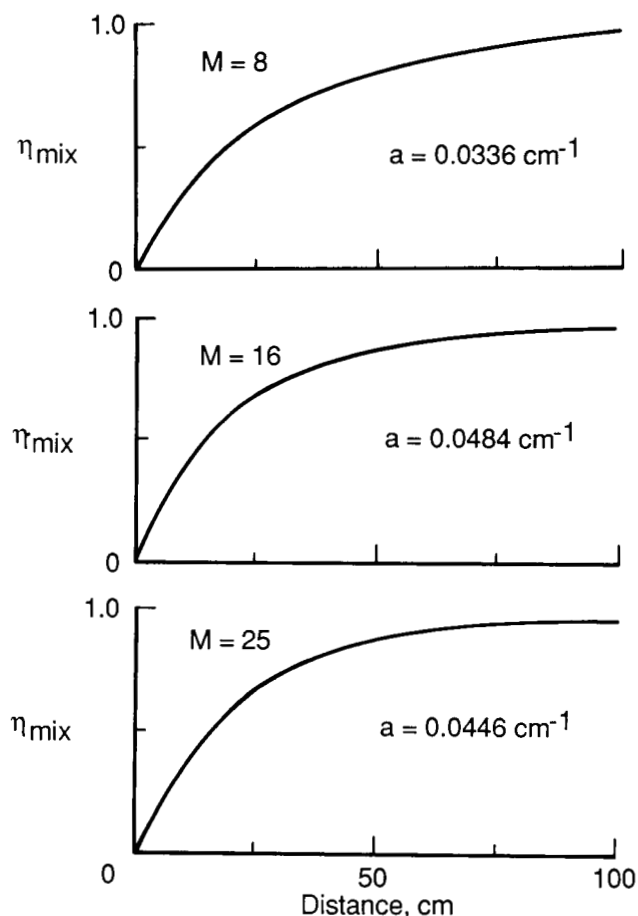


Figure 9. Mixing schedules for each Mach number.

the equivalence ratio is greater than one, the ignition source fraction is defined as the fraction of the total amount of air that is allowed to react to equilibrium with a stoichiometric amount of hydrogen. The purpose of the ignition source is to simulate a flame-holding region that develops around the fuel injector or behind a step in the combustor. From a modelling perspective the ignition source material was assumed to adiabatically mix with remaining fuel and air, a condition which results in an initial mixture with a higher temperature and the presence of free radicals. The mixing schedules given in figure 9 are used for the remaining fuel and air.

The results in figure 10 show that for the Mach 8 condition an ignition source fraction of about 0.1 was required to achieve a reasonable chemical kinetic efficiency near 0.9. For the Mach 16 and Mach 25 conditions the presence of an ignition source did not result in a significant increase in the chemical kinetic efficiency. For these conditions the initial temperature and pressure were high enough to allow self-ignition to occur. For the Mach 25 condition sufficient oxygen atoms were present in the air and

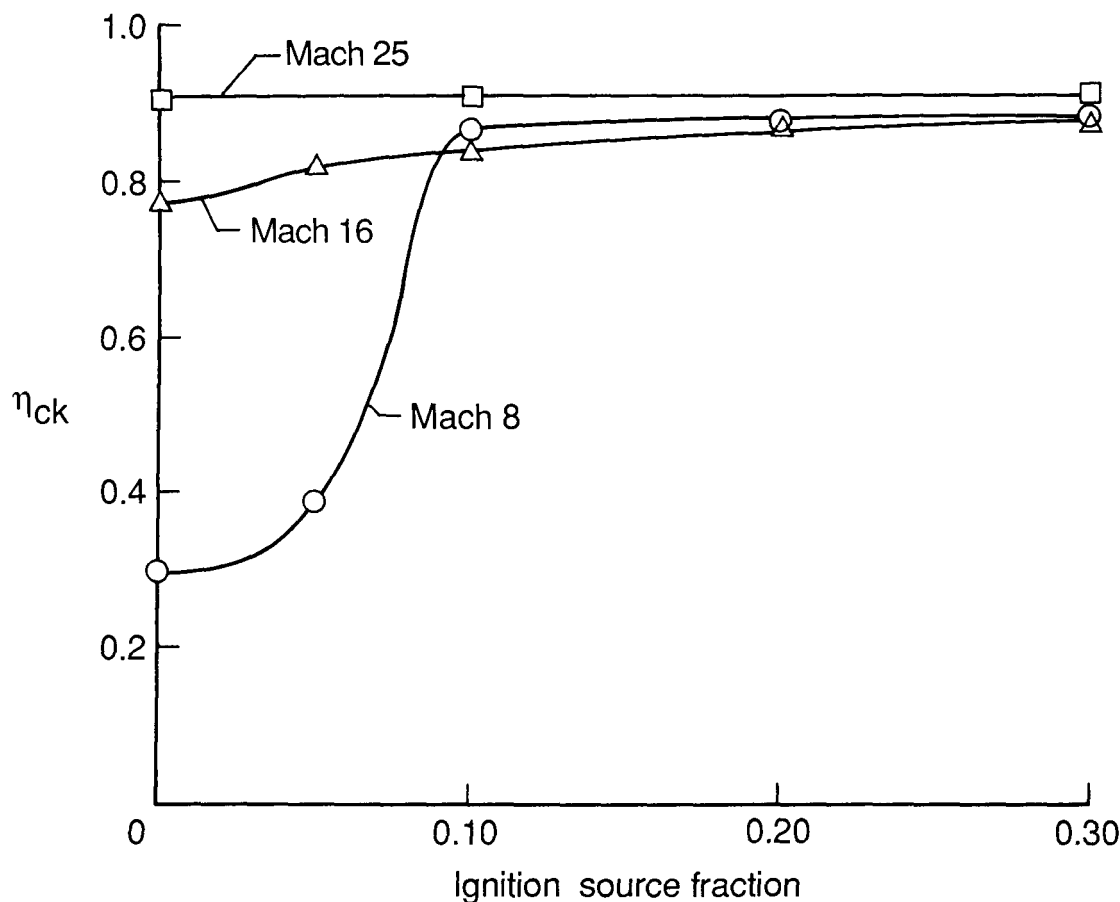


Figure 10. Effect of ignition source fraction on chemical kinetic efficiency.

the additional free radicals provided by the ignition source had a very small effect on the chemistry.

It is evident from the results shown in figure 10 that chemical kinetic effects were present because the chemical kinetic efficiency was less than 1.0 at the conditions examined. To determine which reaction processes were responsible for the kinetic limitations, a parametric study was performed in which the rate coefficients for certain reactions were varied within specified limits. Initially, we varied the rates of various groups of reactions rather than the rates of individual reactions. The groups that were considered included reactions (2) to (5),

- (2) $\text{H} + \text{O}_2 \rightarrow \text{OH} + \text{O}$
- (3) $\text{O} + \text{H}_2 \rightarrow \text{OH} + \text{H}$
- (4) $\text{OH} + \text{H}_2 \rightarrow \text{H}_2\text{O} + \text{H}$
- (5) $\text{OH} + \text{OH} \rightarrow \text{H}_2\text{O} + \text{O}$

which are the primary chain branching and propagating reactions; reactions (6) to (8) and (20),

- (6) $\text{H} + \text{OH} + \text{M} \rightarrow \text{H}_2\text{O} + \text{M}$
- (7) $\text{H} + \text{H} + \text{M} \rightarrow \text{H}_2 + \text{M}$
- (8) $\text{H} + \text{O} + \text{M} \rightarrow \text{OH} + \text{M}$
- (20) $\text{O} + \text{O} + \text{M} \rightarrow \text{O}_2 + \text{M}$

which are the primary recombination reactions; and reaction (9)

- (9) $\text{H} + \text{O}_2 + \text{M} \rightarrow \text{HO}_2 + \text{M}$

which is the primary source of HO_2 in the hydrogen-air reaction mechanism. Reactions involving HO_2 were important in both the ignition delay calculations and the burning velocity calculations. The parametric studies were carried out for hydrogen-air mixtures with an ignition source fraction of 0.10. The results of the studies are shown in figures 11 to 13. In the figures the temperature distributions along the combustor are plotted for the various cases. Results are given for cases in which the rate coefficients in

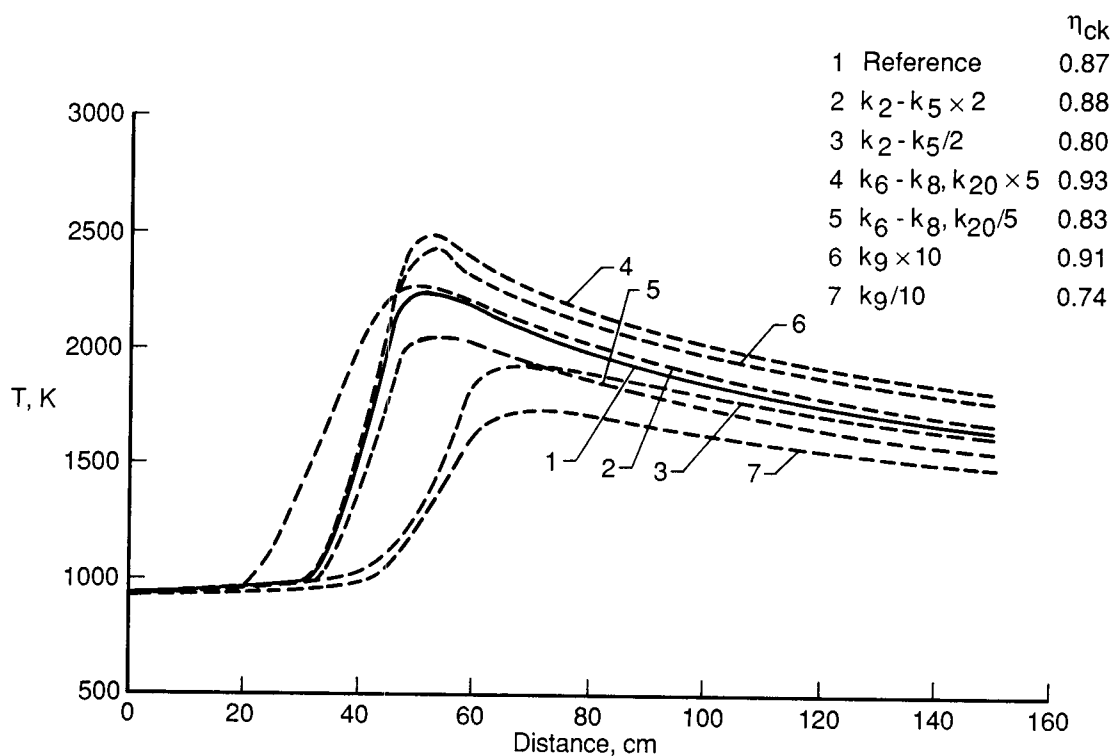


Figure 11. Chemical kinetic effects at Mach 8 condition for $\phi = 1$ and ignition source fraction of 0.10.

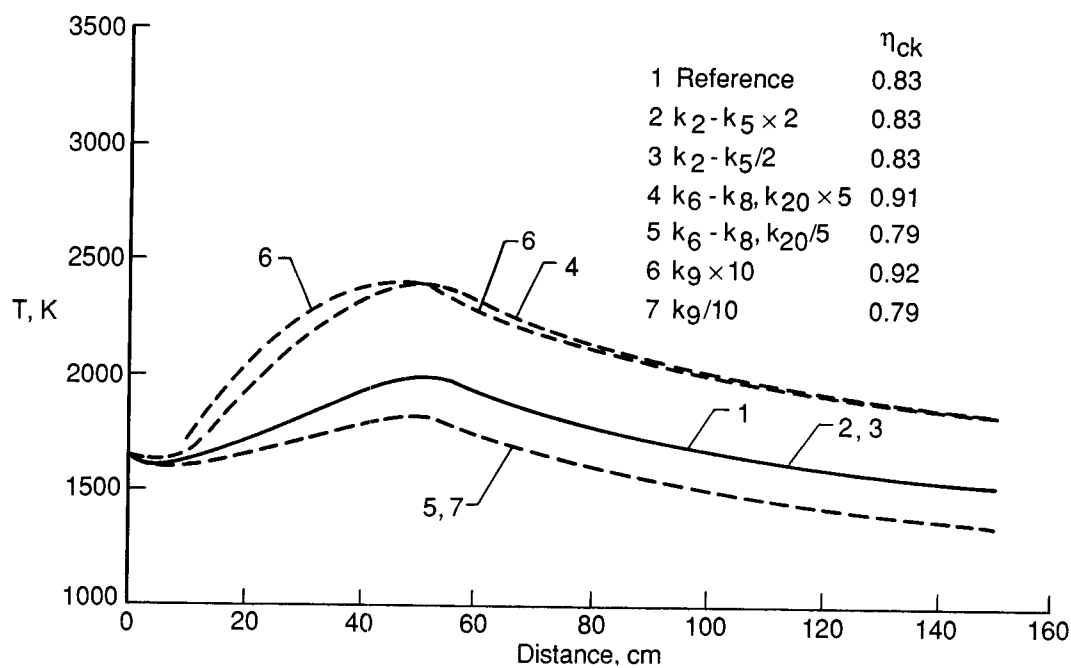


Figure 12. Chemical kinetic effects at Mach 16 condition for $\phi = 1$ and ignition source of 0.10.

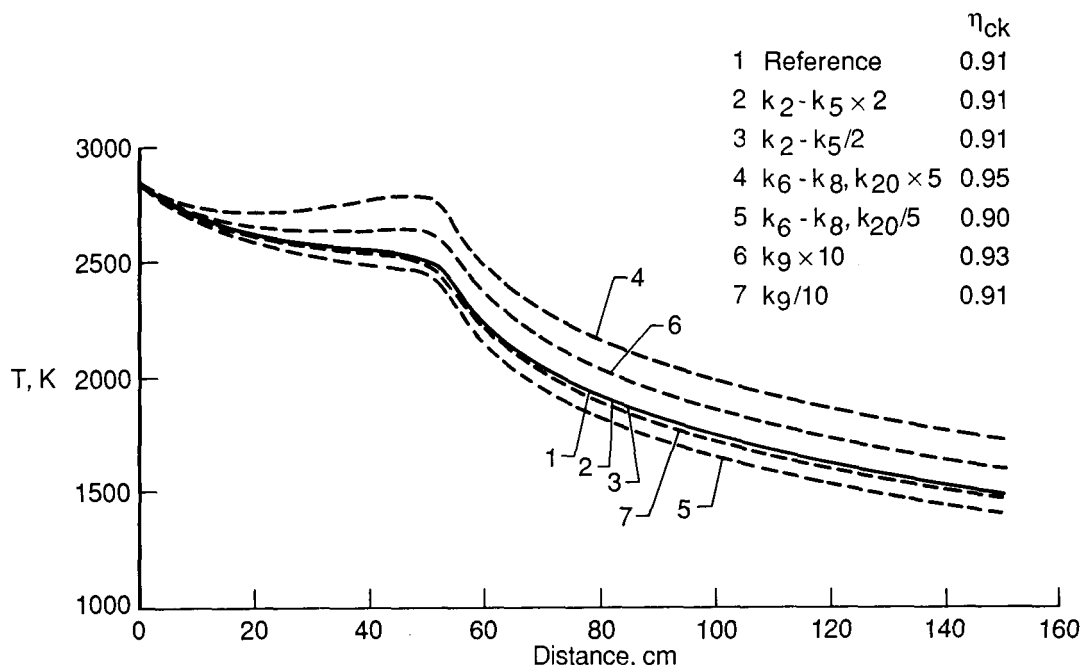
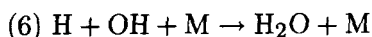


Figure 13. Chemical kinetic effects at Mach 25 condition for $\phi = 2$ and ignition source of 0.10.

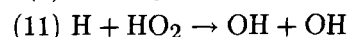
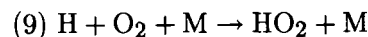
table I for reactions (2) to (5) were varied by a factor of 2, those for the recombination reactions (6) to (8) and (20) were varied by a factor of 5, and that for reaction (9) was varied by a factor of 10. Also shown in each figure is the chemical kinetic efficiency for each case. The reference case in each figure refers to the result obtained with the rate coefficients given in table I.

The results for the Mach 8 condition are shown in figure 11. The results show that all the reactions examined were important and contributed to the kinetic effect. It is evident that at the Mach 8 condition there was an ignition delay which was controlled primarily by the rates of reactions (2) to (5). A decrease in the rate of these reactions produced a significant decrease in the chemical kinetic efficiency, whereas an increase in the reaction rates produced only a slight increase in the chemical kinetic efficiency. Variation of the rates of the recombination reactions (6) to (8) and (20) also influenced the chemical kinetic efficiency. The results of additional parametric studies revealed that the recombination reactions had the largest effect in the combustor section, with reaction (6)

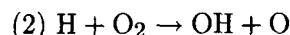


having the largest influence. Variation of the recombination rates in the nozzle section did not produce significant changes in the chemical kinetic efficiency even though some reaction continued in this section.

A significant result of the Mach 8 study was the demonstration that the HO_2 chemistry was an important element in the reaction mechanism. A reduction in the rate of reaction (9) by a factor of 10 (see curve 7 of fig. 11) produced a 15-percent decrease in the chemical kinetic efficiency, while an increase in the rate by a factor of 10 produced a 5-percent increase in the chemical kinetic efficiency. This effect can be explained in terms of reactions (9) and (11):

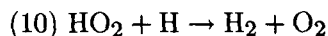


Reaction (9) is the primary source of the HO_2 radical and reaction (11) is the primary chain branching reaction involving the HO_2 radical. Reducing the rate of reaction (9) results in less HO_2 production and, consequently, less chain branching. In addition, reactions (9) and (11) are exothermic; therefore, a reduction in reaction (9) results in less heat release and consequently a lower temperature, which affects the rate of the important endothermic chain branching reaction



When the rate of reaction (9) is increased, the effect on the chemical kinetic efficiency is not as large as the effect when the rate of reaction (9) is decreased because even though more HO_2 radical is produced, the conversion of HO_2 to OH is limited by the rate

of reaction (11) and competition from reactions (10) and (14)



For the Mach 8 condition the HO_2 chemistry is important primarily in the combustor section and is less important in the nozzle section, even though the reactions continue.

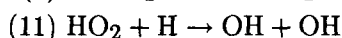
The results for the Mach 16 condition are shown in figure 12. For this condition, varying the rates of reactions (2) to (5) did not affect the chemical kinetic efficiency, and this lack of effect indicates the overall combustion process was controlled by other reactions. The recombination reactions (6) to (8) and reaction (9) had the largest influence on the combustion process and this effect primarily occurred in the combustor section. In the nozzle section the kinetics of the three-body reactions were essentially frozen while the two-body reactions continued. The results given in figure 12 again illustrate the importance of the HO_2 chemistry and the need to include the HO_2 chemistry in the mechanism.

The results for the Mach 25 condition are shown in figure 13. Varying the rates of reactions (2) to (5) did not affect the chemical kinetic efficiency. The results of additional studies revealed that the controlling reactions in the combustor were the recombination reactions (6) to (8), with reaction (6) being the most important in the combustor section. In the nozzle section the recombination reactions were virtually frozen.

Discussion of Results

The results of the study suggest that chemical kinetic effects can be important at representative scramjet combustor conditions and that combustor models which use nonequilibrium chemistry are preferable to models that assume equilibrium chemistry. For the conditions examined the results also show the importance of including the HO_2 chemistry in the mechanism. Results obtained with a simplified model that does not include the HO_2 chemistry can be significantly different from the results obtained with a model that includes HO_2 chemistry. This difference is illustrated in figures 14 and 15, which show the temperature profile and the chemical kinetic efficiency for the Mach 8 and Mach 16 conditions. The solid curves are the results based on the reaction mechanism and the rate coefficients listed in table I. For the Mach 8 condition omitting the HO_2 and H_2O_2 reactions from the model resulted in a 29-percent reduction in the chemical kinetic efficiency, while for the Mach 16 condition there was a

6-percent reduction. The reactions primarily responsible for this effect were reactions (9) and (11),



which contributed to the production of free radicals and the release of energy. This effect was very evident for the Mach 8 condition, for which the ignition process was delayed and did not take place in the combustor section. Reaction still occurred in the nozzle section because the rate coefficient for reaction (9) increased with decreasing temperatures and the rate of reaction (11) was not a strong function of temperature. At the Mach 25 condition, omitting the HO_2 reactions did not affect the results.

Thus far the discussion of the chemical kinetic effects has centered on the effects of groups of reactions on the calculated behavior of the hydrogen-air system. Another aspect that needs to be considered is the matter of the effect of the uncertainty in the assigned rate coefficients on the calculated results. Baulch et al. (1972) and Baulch, Drysdale, and Horne (1973) have evaluated the rate coefficient data for most of the reactions in the hydrogen-oxygen mechanism and assigned error or uncertainty limits which ranged from ± 20 percent to a factor of three. With such errors the predictive capability of the mechanism might be questioned. This would be the case if the mechanism were assembled arbitrarily without comparison or optimization with experimental data. By optimizing the mechanism with experimental data, we can assemble a mechanism with an internally consistent set of rate coefficients that can be defined to within rather narrow limits. The reaction mechanism proposed in this report was optimized through comparison of calculated ignition delay times and burning velocities with experimental data. The resulting mechanism could reproduce the experimental results to within ± 20 percent. As part of the optimization procedure, a reaction rate sensitivity analysis was performed in which the rate coefficients for all the reactions were varied within the error limits suggested by Baulch, Drysdale, and Horne (1973) and by Dixon-Lewis (1979). This analysis revealed that the calculated ignition delay times and burning velocities were the most sensitive to the rate coefficients assigned to reactions (2) to (5), (9) to (15), and (6) to (8), in that order. Additional studies showed that varying the rate coefficients for reactions (2) to (5) and (9) by more than 10 percent about the values given by the expressions in table I gave calculated results that were not in good agreement with the experimental data. Similar studies with reactions (10) to (15) showed that variations of

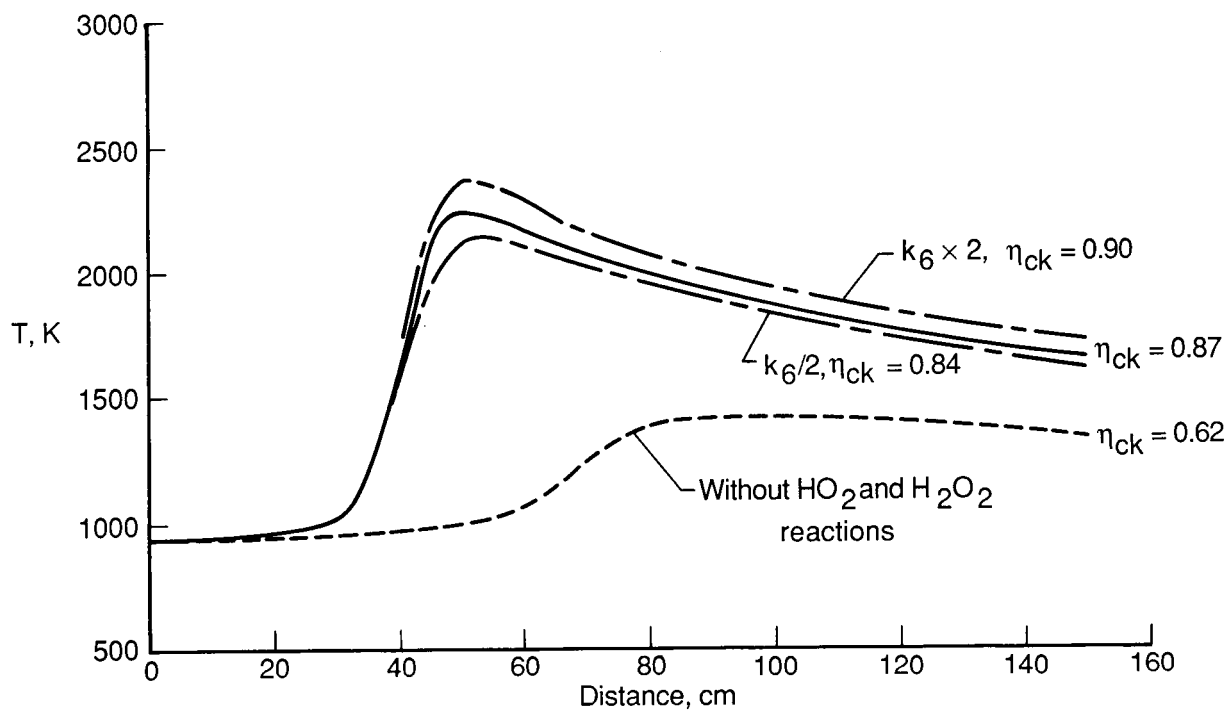


Figure 14. Effect of HO_2 and H_2O_2 reactions at Mach 8 condition.

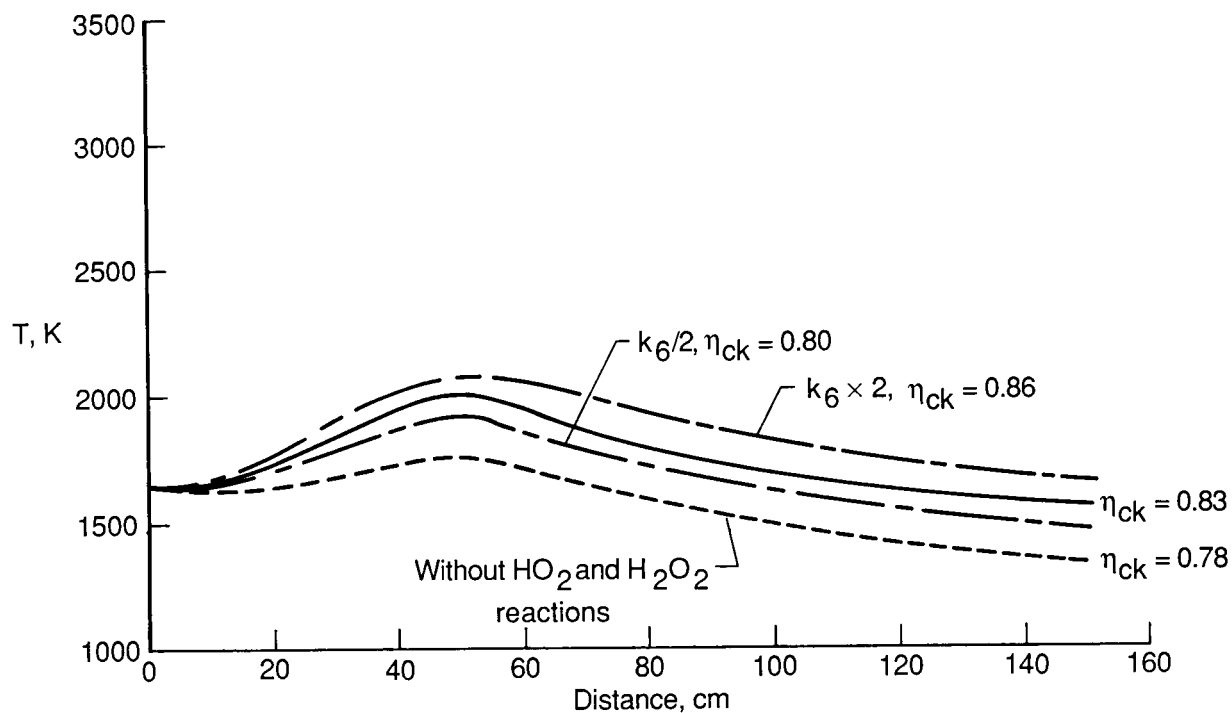


Figure 15. Effect of HO_2 and H_2O_2 reactions at Mach 16 condition.

± 50 percent were acceptable. Varying the rate coefficients for reactions (16) to (19) by a factor up to two did not significantly alter the calculated results. The most important recombination reaction, after reaction (9), is reaction (6). The rate coefficient for reaction (6) could be varied to within a factor of two without significantly affecting the calculated results. The rate coefficient for the other recombination reactions (7), (8), and (20) could be varied to within a factor of five and still provide satisfactory agreement between the calculated and experimental results. The sensitivity of the calculated results to the nitrogen-oxygen chemistry represented by reactions (21) to (33) was also examined. The calculated ignition delay times for the H_2 -NO- O_2 - N_2 mixtures (fig. 3) were very sensitive to the rate coefficient assigned to reaction (30). Varying the rate coefficient for reaction (30) by ± 50 percent did not significantly alter the results. The rate coefficients for the other reactions could be varied to at least a factor of two without significantly affecting the calculated results.

Based on the results of the sensitivity study it was concluded that for the reaction mechanism given in table I, the uncertainties associated with the various rate coefficients are the following: for reaction (1), a factor of five; for reactions (2) to (5) and (9), ± 10 percent; for reaction (6), a factor of two; for reactions (7), (8), and (20), a factor of five; for reactions (10) to (15) and (30), ± 50 percent; and for the remaining reactions, a factor of two. With these uncertainties only the variation in the rate coefficient for reaction (6), the recombination of H and OH to form H_2O , would have an effect on calculated results for the Mach 8 and Mach 16 conditions. Varying the rate of reaction (6) by a factor of two produced a 4-percent change in the chemical kinetic efficiency, as shown in figures 14 and 15. At the Mach 25 condition, varying the rate of reaction (6) by a factor of two did not influence the calculated results.

Concluding Remarks

A chemical kinetic mechanism for the combustion of hydrogen has been assembled and optimized through comparison of the observed behavior determined in shock-tube and flame studies with behavior predicted by the mechanism. The reactions contained in the mechanism reflect the current state of knowledge of the chemistry of the hydrogen-air system, and the assigned rate coefficients are consistent with accepted values reported in the literature. It was determined that the mechanism is capable of satisfactorily reproducing the experimental results for a range of conditions relevant to scramjet combustion.

Calculations made with the reaction mechanism for representative scramjet combustor conditions at

Mach 8, 16, and 25 gave the following results. Chemical kinetic effects are important and result in a decrease in internal thrust compared with the equilibrium chemistry condition. For Mach numbers less than 16, the studies suggest that an ignition source will most likely be required to overcome the slow ignition chemistry at these conditions. At the Mach 25 condition, the initial temperature and pressure were high enough so that ignition was rapid and the presence of an ignition source did not significantly affect reaction rates. Most of the combustion process occurred in the combustor section. At the Mach 8 condition the overall reaction rate is controlled by the rates of the chain propagating and branching reactions, the recombination reactions, and the HO_2 -consuming reactions. At the Mach 16 condition the recombination reactions and the HO_2 -consuming reactions are the rate controlling processes. At the Mach 25 condition the rate of the recombination reaction controls the combustion process.

NASA Langley Research Center
Hampton, VA 23665-5225
December 22, 1987

References

- Anderson, Griffin Y. 1974: An Examination of Injector/Combustor Design Effects on Scramjet Performance. NASA paper presented at the 2nd International Symposium on Air Breathing Engines (Sheffield, England), Mar. 25-29.
- Anderson, Griffin Y.; and Rogers, R. Clayton 1971: *A Comparison of Experimental Supersonic Combustor Performance With an Empirical Correlation of Nonreactive Mixing Results*. NASA TM X-2429.
- Bartlett, Eugene P.; Kendall, Robert M.; and Rindal, Roald A. 1968: *An Analysis of the Coupled Chemically Reacting Boundary Layer and Charring Ablator. Part IV—A Unified Approximation for Mixture Transport Properties for Multicomponent Boundary-Layer Applications*. NASA CR-1063.
- Baulch, D. L.; Drysdale, D. D.; Horne, D. G.; and Lloyd, A. C. c.1972: *Evaluated Kinetic Data for High Temperature Reactions. Volume 1—Homogeneous Gas Phase Reactions of the H_2 - O_2 System*. CRC Press.
- Baulch, D. L.; Drysdale, D. D.; and Horne, D. G. c.1973: *Evaluated Kinetic Data for High Temperature Reactions. Volume 2—Homogeneous Gas Phase Reactions of the H_2 - N_2 - O_2 System*. Butterworth & Co. (Publ.), Ltd.
- Bittker, David A.; and Scullin, Vincent J. 1972: *General Chemical Kinetics Computer Program for Static and Flow Reactions, With Application to Combustion and Shock-Tube Kinetics*. NASA TN D-6586.
- Dixon-Lewis, G.; and Williams, D. J. 1977: The Oxidation of Hydrogen and Carbon Monoxide. *Comprehensive*

- Chemical Kinetics*, C. H. Bamford and C. F. H. Tipper, eds., Volume 17 of Gas-Phase Combustion, Elsevier Scientific Publ. Co., pp. 1-248.
- Dixon-Lewis, G. 1979: Kinetic Mechanism, Structure and Properties of Premixed Flames in Hydrogen-Oxygen-Nitrogen Mixtures. *Philos. Trans. Royal Soc. London*, vol. 292, no. 1388, Aug. 24, pp. 45-99.
- Dougherty, Eugene P.; and Rabitz, Herschel 1980: Computational Kinetics and Sensitivity Analysis of Hydrogen-Oxygen Combustion. *J. Chem. Phys.*, vol. 72, no. 12, June 15, pp. 6571-6586.
- Gay, A.; and Pratt, N. H. c.1971: Hydrogen-Oxygen Recombination Measurements in a Shock Tube Steady Expansion. *Shock Tube Research—Proceedings of the Eighth International Shock Tube Symposium*, J. L. Stollery, A. G. Gaydon, and P. R. Owen, eds., Chapman and Hall Ltd., pp. 39/1-39/13.
- JANAF Thermochemical Tables, Second ed. 1971. NSRDS-NBS 37, U.S. Dep. of Commerce, June.
- Kendall, Robert M.; and Kelly, John T. 1978: *Premixed One-Dimensional Flame (PROF) Code User's Manual*. EPA-600/7-78-172a, U.S. Environmental Protection Agency, Aug.
- McLain, Allen G.; and Rao, C. S. R. 1976: *A Hybrid Computer Program for Rapidly Solving Flowing or Static Chemical Kinetic Problems Involving Many Chemical Species*. NASA TM X-3403.
- Milton, B. E.; and Keck, J. C. 1984: Laminar Burning Velocities in Stoichiometric Hydrogen and Hydrogen-Hydrocarbon Gas Mixtures. *Combust. & Flame*, vol. 58, no. 1, Oct., pp. 13-22.
- Slack, M. W. 1977: Rate Coefficient for $H + O_2 + M = HO_2 + M$ Evaluated From Shock Tube Measurements of Induction Times. *Combust. & Flame*, vol. 28, no. 3, pp. 241-249.
- Slack, M.; and Grillo, A. 1977: *Investigation of Hydrogen-Air Ignition Sensitized by Nitric Oxide and by Nitrogen Dioxide*. NASA CR-2896.
- Warnatz, Jürgen 1981: Concentration-, Pressure-, and Temperature-Dependence of the Flame Velocity in Hydrogen-Oxygen-Nitrogen Mixtures. *Combust. Sci. & Technol.*, vol. 26, nos. 5 and 6, pp. 203-213.

Table I. Hydrogen-Air Combustion Mechanism^a

Reaction ^b	A	n	E
(1) $\text{H}_2 + \text{O}_2 \rightarrow \text{OH} + \text{OH}$	1.70×10^{13}	0	48 000
(2) $\text{H} + \text{O}_2 \rightarrow \text{OH} + \text{O}$	2.60×10^{14}	0	16 800
(3) $\text{O} + \text{H}_2 \rightarrow \text{OH} + \text{H}$	1.80×10^{10}	1.00	8 900
(4) $\text{OH} + \text{H}_2 \rightarrow \text{H}_2\text{O} + \text{H}$	2.20×10^{13}	0	5 150
(5) $\text{OH} + \text{OH} \rightarrow \text{H}_2\text{O} + \text{O}$	6.30×10^{12}	0	1 090
(6) $\text{H} + \text{OH} + \text{M} \rightarrow \text{H}_2\text{O} + \text{M}$	2.20×10^{22}	-2.00	0
(7) $\text{H} + \text{H} + \text{M} \rightarrow \text{H}_2 + \text{M}$	6.40×10^{17}	-1.00	0
(8) $\text{H} + \text{O} + \text{M} \rightarrow \text{OH} + \text{M}$	6.00×10^{16}	-.6	0
(9) $\text{H} + \text{O}_2 + \text{M} \rightarrow \text{HO}_2 + \text{M}$	2.10×10^{15}	0	-1 000
(10) $\text{HO}_2 + \text{H} \rightarrow \text{H}_2 + \text{O}_2$	1.30×10^{13}	0	0
(11) $\text{HO}_2 + \text{H} \rightarrow \text{OH} + \text{OH}$	1.40×10^{14}	0	1 080
(12) $\text{HO}_2 + \text{H} \rightarrow \text{H}_2\text{O} + \text{O}$	1.00×10^{13}	0	1 080
(13) $\text{HO}_2 + \text{O} \rightarrow \text{O}_2 + \text{OH}$	1.50×10^{13}	0	950
(14) $\text{HO}_2 + \text{OH} \rightarrow \text{H}_2\text{O} + \text{O}_2$	8.00×10^{12}	0	0
(15) $\text{HO}_2 + \text{HO}_2 \rightarrow \text{H}_2\text{O}_2 + \text{O}_2$	2.00×10^{12}	0	0
(16) $\text{H} + \text{H}_2\text{O}_2 \rightarrow \text{H}_2 + \text{HO}_2$	1.40×10^{12}	0	3 600
(17) $\text{O} + \text{H}_2\text{O}_2 \rightarrow \text{OH} + \text{HO}_2$	1.40×10^{13}	0	6 400
(18) $\text{OH} + \text{H}_2\text{O}_2 \rightarrow \text{H}_2\text{O} + \text{HO}_2$	6.10×10^{12}	0	1 430
(19) $\text{M} + \text{H}_2\text{O}_2 \rightarrow \text{OH} + \text{OH} + \text{M}$	1.20×10^{17}	0	45 500
(20) $\text{O} + \text{O} + \text{M} \rightarrow \text{O}_2 + \text{M}$	6.00×10^{17}	0	-1 800
(21) $\text{N} + \text{N} + \text{M} \rightarrow \text{N}_2 + \text{M}$	2.80×10^{17}	-.75	0
(22) $\text{N} + \text{O}_2 \rightarrow \text{NO} + \text{O}$	6.40×10^9	1.00	6 300
(23) $\text{N} + \text{NO} \rightarrow \text{N}_2 + \text{O}$	1.60×10^{13}	0	0
(24) $\text{N} + \text{OH} \rightarrow \text{NO} + \text{H}$	6.30×10^{11}	.50	0
(25) $\text{H} + \text{NO} + \text{M} \rightarrow \text{HNO} + \text{M}$	5.40×10^{15}	0	-600
(26) $\text{H} + \text{HNO} \rightarrow \text{NO} + \text{H}_2$	4.80×10^{12}	0	0
(27) $\text{O} + \text{HNO} \rightarrow \text{NO} + \text{OH}$	5.00×10^{11}	.50	0
(28) $\text{OH} + \text{HNO} \rightarrow \text{NO} + \text{H}_2\text{O}$	3.60×10^{13}	0	0
(29) $\text{HO}_2 + \text{HNO} \rightarrow \text{NO} + \text{H}_2\text{O}_2$	2.00×10^{12}	0	0
(30) $\text{HO}_2 + \text{NO} \rightarrow \text{NO}_2 + \text{OH}$	3.40×10^{12}	0	-260
(31) $\text{H} + \text{NO}_2 \rightarrow \text{NO} + \text{OH}$	3.50×10^{14}	0	1 500
(32) $\text{O} + \text{NO}_2 \rightarrow \text{NO} + \text{O}_2$	1.00×10^{13}	0	600
(33) $\text{M} + \text{NO}_2 \rightarrow \text{NO} + \text{O} + \text{M}$	1.16×10^{16}	0	66 000

^aThe rate coefficients are given in the form $k = AT^n \exp(-E/RT)$; units are in seconds, moles, cubic centimeters, calories, and kelvins.

^bThe third-body efficiencies relative to $\text{N}_2 = 1.0$ are as follows: for reaction (6), $\text{H}_2\text{O} = 6.0$; for reaction (7), $\text{H}_2 = 2.0$ and $\text{H}_2\text{O} = 6.0$; for reaction (8), $\text{H}_2\text{O} = 5.0$; for reaction (9), $\text{H}_2 = 2.0$ and $\text{H}_2\text{O} = 16.0$; and for reaction (19), $\text{H}_2\text{O} = 15.0$.

Table II. Initial Combustor Conditions

M	ϕ	T, K	p, atm	$V, \text{m/sec}$
8	1.0	670	0.50	2090
16	1.0	1500	.90	4658
25	2.0	2800	1.40	7571



National Aeronautics and
Space Administration

Report Documentation Page

1. Report No. NASA TP-2791	2. Government Accession No.	3. Recipient's Catalog No.	
4. Title and Subtitle An Analytical Study of the Hydrogen-Air Reaction Mechanism With Application to Scramjet Combustion		5. Report Date February 1988	
		6. Performing Organization Code	
7. Author(s) Casimir J. Jachimowski		8. Performing Organization Report No. L-16372	
		10. Work Unit No. 505-62-31-01	
9. Performing Organization Name and Address NASA Langley Research Center Hampton, VA 23665-5225		11. Contract or Grant No.	
		13. Type of Report and Period Covered Technical Paper	
12. Sponsoring Agency Name and Address National Aeronautics and Space Administration Washington, DC 20546-0001		14. Sponsoring Agency Code	
15. Supplementary Notes			
16. Abstract A chemical kinetic mechanism for the combustion of hydrogen is assembled and optimized through comparison of the observed behavior determined in shock-tube and flame studies with behavior predicted by the mechanism. The reactions contained in the mechanism reflect the current state of knowledge of the chemistry of the hydrogen-air system, and the assigned rate coefficients are consistent with accepted values reported in the literature. The mechanism is capable of satisfactorily reproducing the experimental results for a range of conditions relevant to scramjet combustion. Calculations made with the reaction mechanism for representative scramjet combustor conditions at Mach 8, 16, and 25 show that chemical kinetic effects can be important and that combustor models which use nonequilibrium chemistry should be used in preference to models which assume equilibrium chemistry. For the conditions examined the results also show the importance of including the HO ₂ chemistry in the mechanism.			
17. Key Words (Suggested by Authors(s)) Kinetic mechanism Supersonic combustion Hydrogen combustion modelling		18. Distribution Statement Unclassified—Unlimited Subject Category 25	
19. Security Classif.(of this report) Unclassified	20. Security Classif.(of this page) Unclassified	21. No. of Pages 16	22. Price A02